10. Stratigraphy of the Dolomites

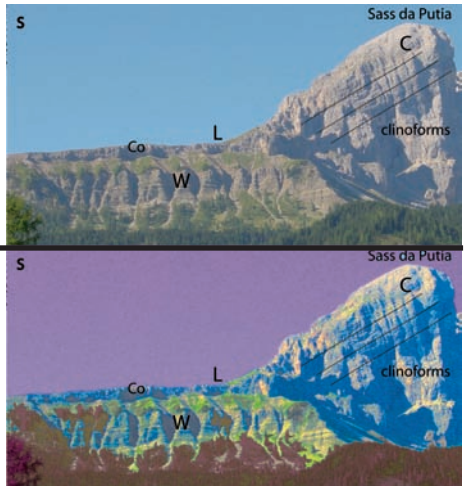

Fig. 195 - Phyllites recording Hercynian deformation in the NW-ward dipping basement of the Dolomites. 3 km south of Agordo. Chris Golding for scale.

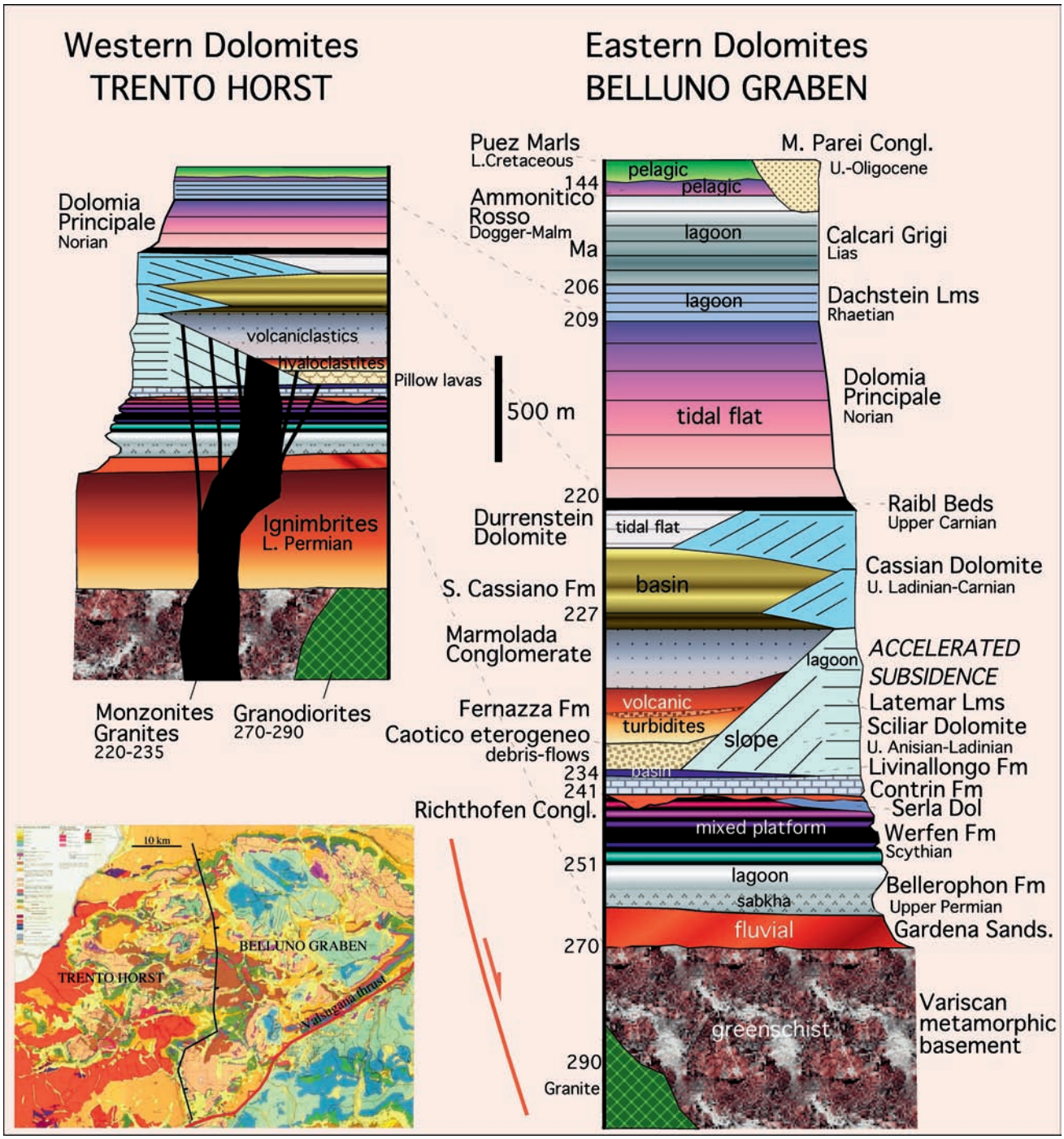

Fig. 196 - General stratigraphy of the Dolomites. The eastern side (Belluno Graben) underwent larger subsidence throughout the entire late Permian-Mesozoic. The differential subsidence was accommodated by a number of synsedimentary, roughly N-S-trending normal faults. The western side (Trento horst) has a thickness reduced to about a half with respect to the Belluno graben. Note that during the late Anisian-early Ladinian, the region had an accelerated subsidence (about 0.6 mm/yr) that allowed the fast aggradation and growth of the Sciliar Dolomite (Marmolada Lms). Most of the Mid-Triassic calcalkaline magmatism (e.g., intrusions of Predazzo and Monzoni) and the lower Permian porphyry (Piastrone porfirico Atesino) concentrated in the Trento horst.

Fig. 197 - Detail of the Permian-Triassic boundary (the largest extinction) in the Dolomites. From the bottom to the top: marls, gypsum and bituminous limestones of the upper Permian Bellerophon Fm (B); the first cliff is constituted by Triassic marly limestones of the Mazzin Member (M) of the Werfen Fm (Scythian); a yellow-orange level marks the occurrence of the evaporitic dolomites of the Andraz Horizon of the Werfen Fm (A); the topmost cliff (Siusi Member of the Werfen Fm, S) is made by marly and oolitic limestones with frequent intercalations (toward the top) of reddish siltstones. The picture was taken at the western end of the Pale di San Martino massif, near Passo Rolle.

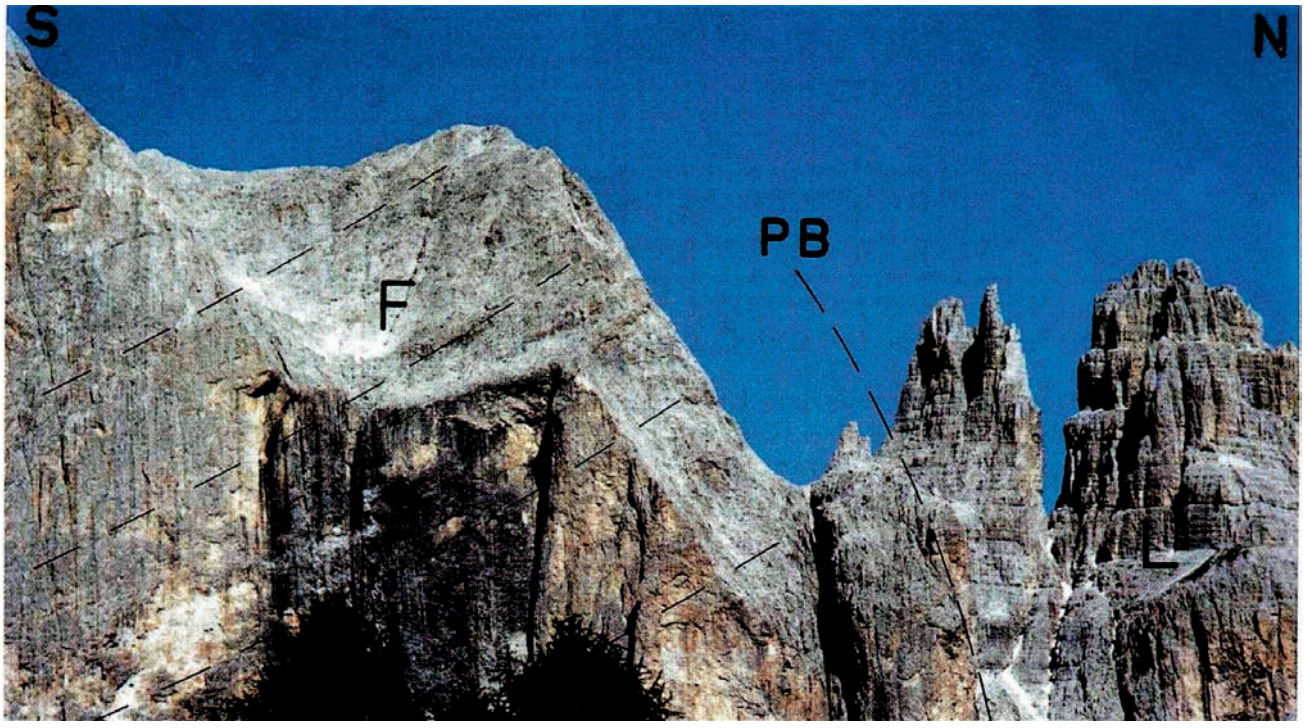

Fig. 198 - Transition (platform break plane, PB) between internal lagoon sediments (back reef, L) and clinostratified escarpment sediments (fore-reef, F) of the Ladinian Marmolada Limestone (or Sciliar Dolomite). The plane is steeply dipping, thus indicating strong aggradation. Photo taken in the Catinaccio Massif.

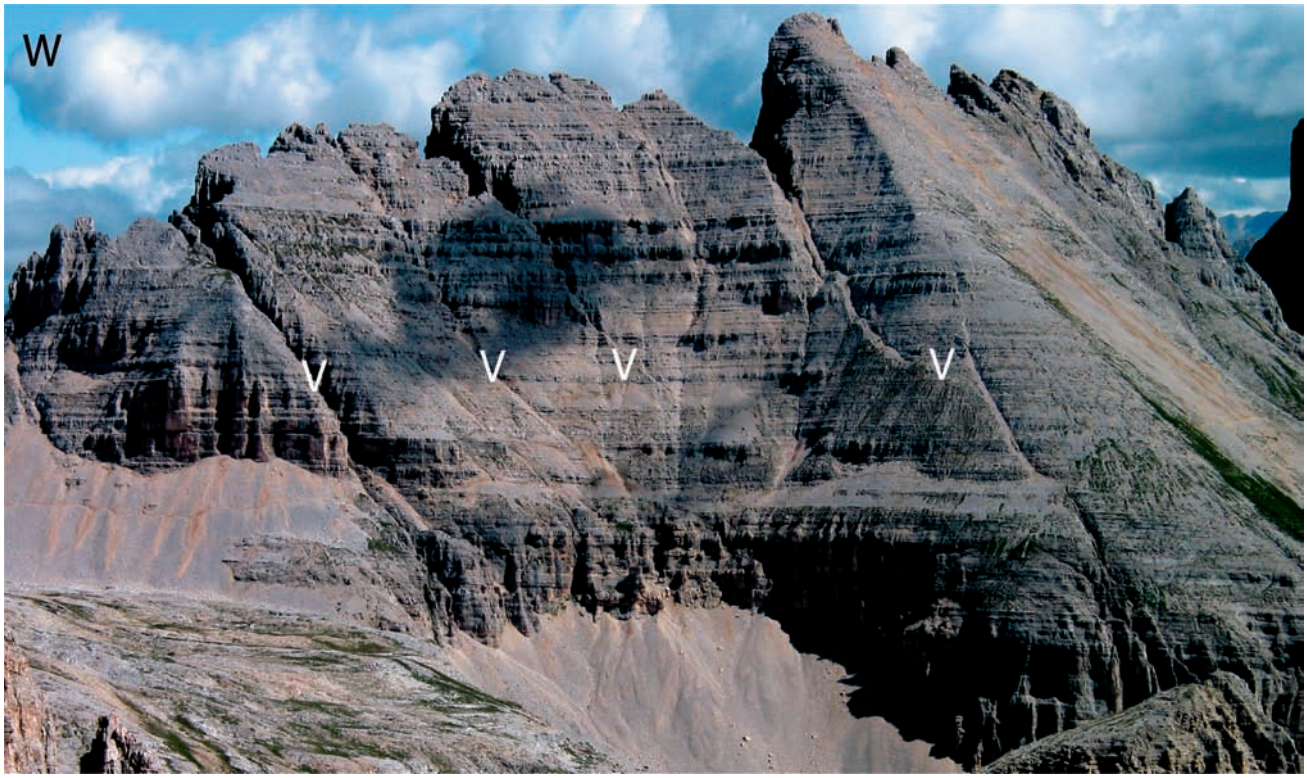

Fig. 199 - Latemar Massif, western Dolomites. The carbonate platform is showing its backreef or lagoon. V, late Ladinian volcanic dikes. There are different datings and genetic interpretations on the evolution of this platform (Gaetani *et alii*, 1981; Goldhammer *et alii*, 1990; Kent *et alii*, 2004). Whatever the interpretation, the subsidence rate can be higher than 0.6 mm/yr, a rate typical of backarc basins associated to W-directed subduction zones.

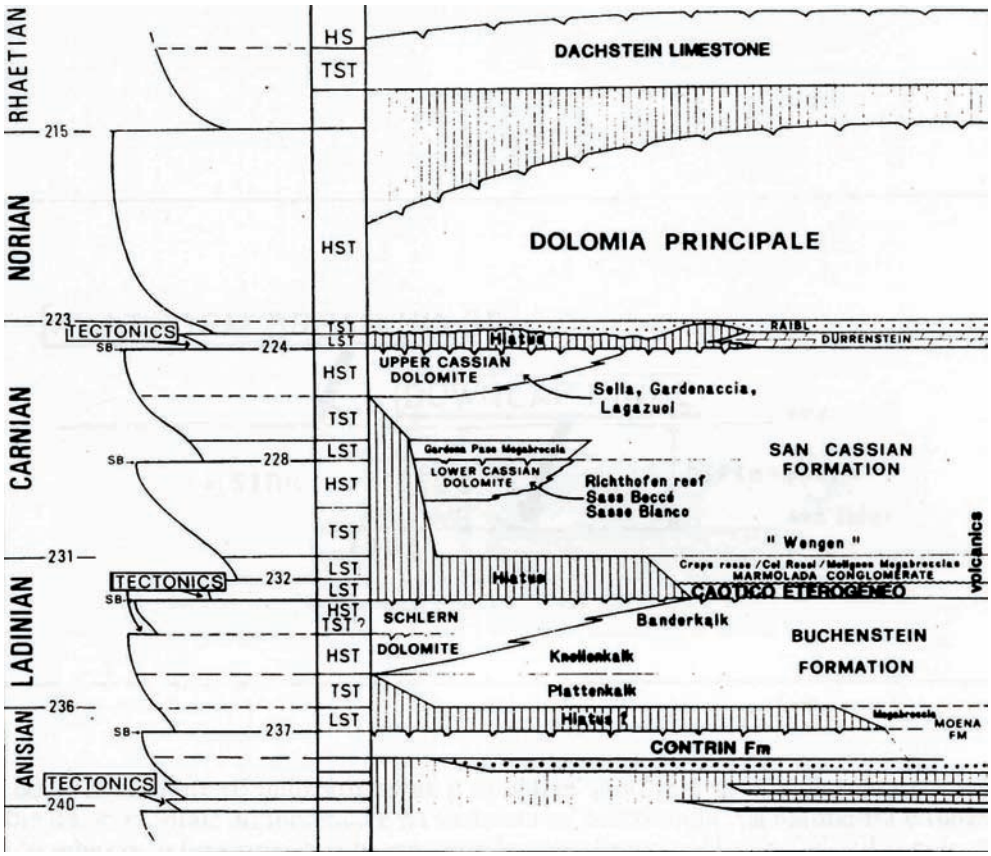

Fig. 200 - Chronostratigraphic chart of the Middle-Upper Triassic of the Dolomites, compared to the coastal onlap curve (after Doglioni *et alii*, 1989a).

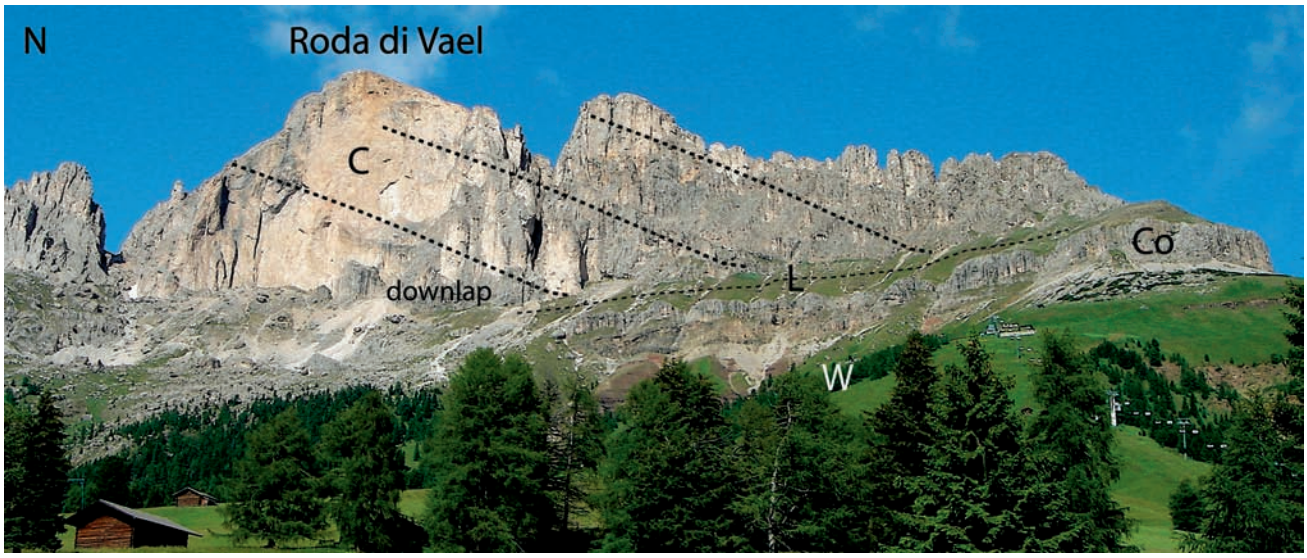

Fig. 201 - View of the southern outcropping termination of the Catinaccio prograding carbonate platform. C, Marmolada Limestone; L, Livinallongo Fm; Co, Contrin Fm; W, Werfen Fm. See next figure.

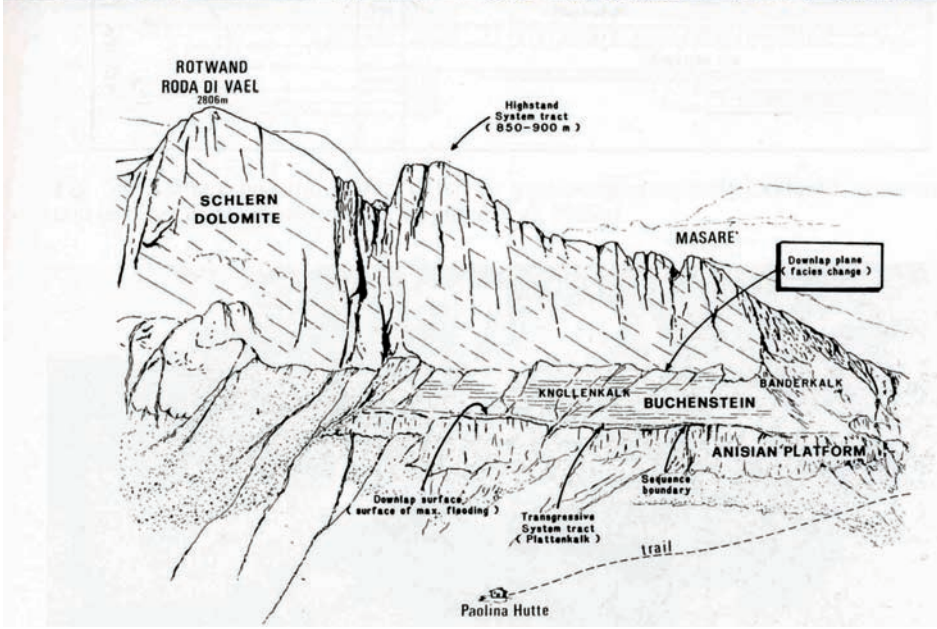

Fig.202 - The Ladinian carbonate platform of the Catinaccio Massif, with its clinostratified megabreccias (D) prograding towards the south (to the right). Notice that the ledge of the Livinallongo Fm (L), made up of basinal sediments eteropic to the platform, reduces and disappears moving to the left, at the core of the platform. Here, internal lagoon deposits directly overlie Anisian platform sediments (C). A syn-sedimentary fault probably accommodated a faster subsidence to the north, at the left margin of the picture above. W, Werfen Fm. The drawing below is the interpretation in terms of sequence stratigraphy of a detail of the southern margin of the picture (after BOSELLINI & DOGLIONI, 1988).

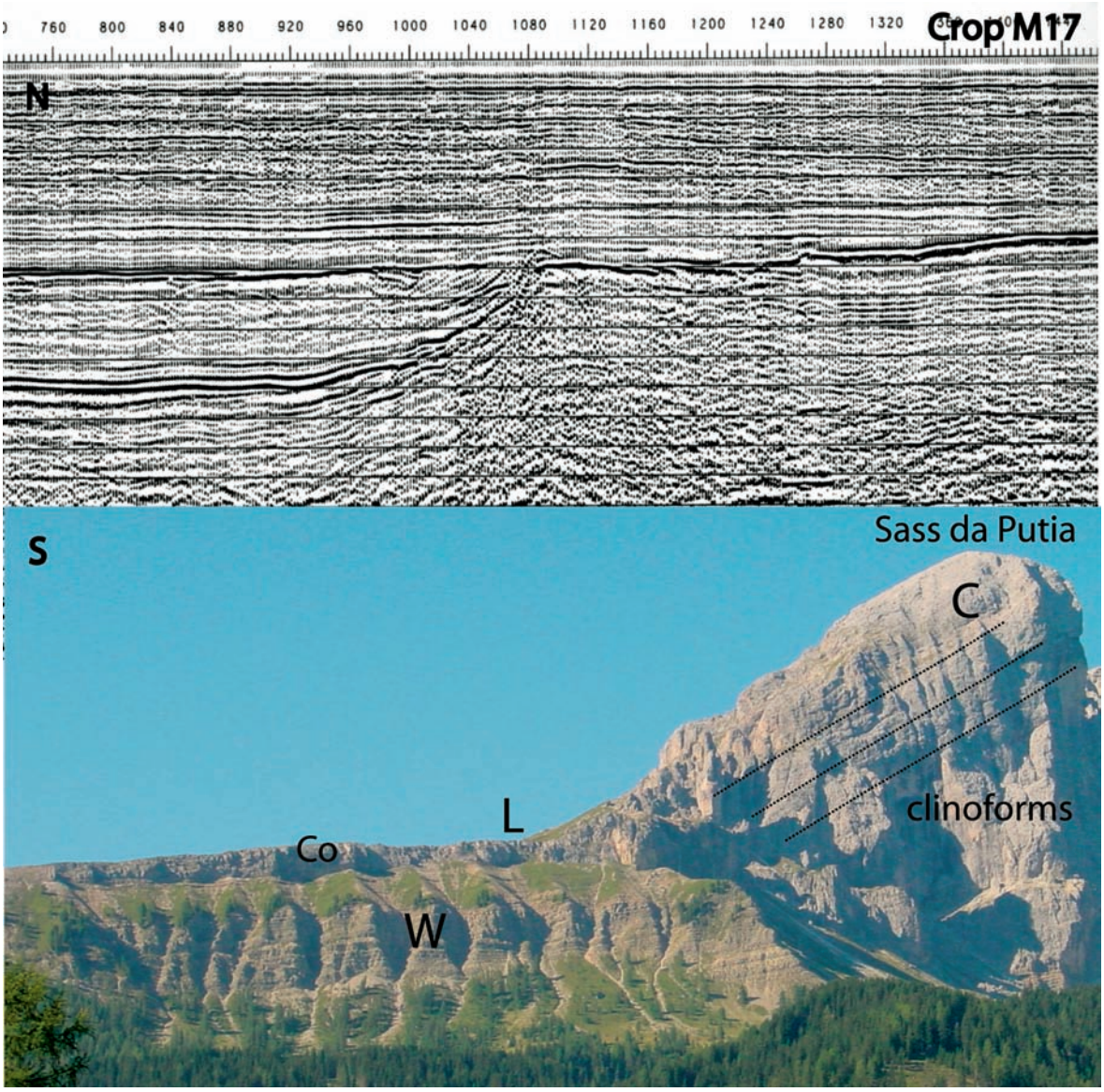

Fig. 203 - Above: seismic reflection profile in the Adriatic Sea (Crop Atlas, Scrocca *et alii*, 2003) crossing the Mesozoic slope of a carbonate platform. Below: outcropping example of prograding margin of a Ladinian carbonate platform (C, Marmolada Limestone), over the basinal equivalent (L, Livinallongo Fm); W, Werfen Fm, Scythian; Co, Contrin Fm, Upper Anisian. Sass da Putia, northern Dolomites.

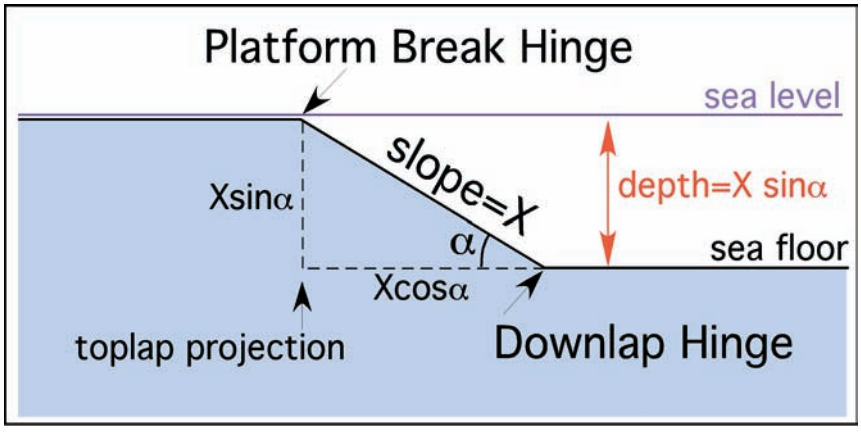

Fig. 204 - Platform break and downlap hinges are the points where stratification changes from horizontal to inclined and from inclined to horizontal. The sea depth is a function of the length of the slope (X) connecting the platform with the basin, and of the angle of the lower slope with the horizontal (α). Thus, Xsinα is almost equal to the depth of the basin, and Xcosα is the distance between the platform break projection and the downlap hinge (after Doglioni & Bosellini, 1989).

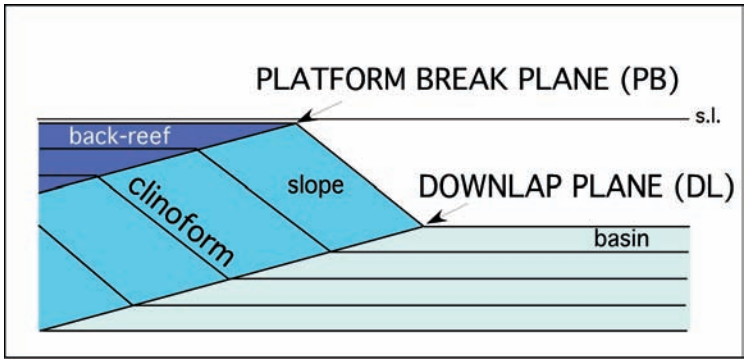

Fig. 205 - The platform break and downlap planes are the ideal planes intersecting respectively all the platform break and the downlap hinges in a progradational system (after DOGLIONI & BOSELLINI, 1989).

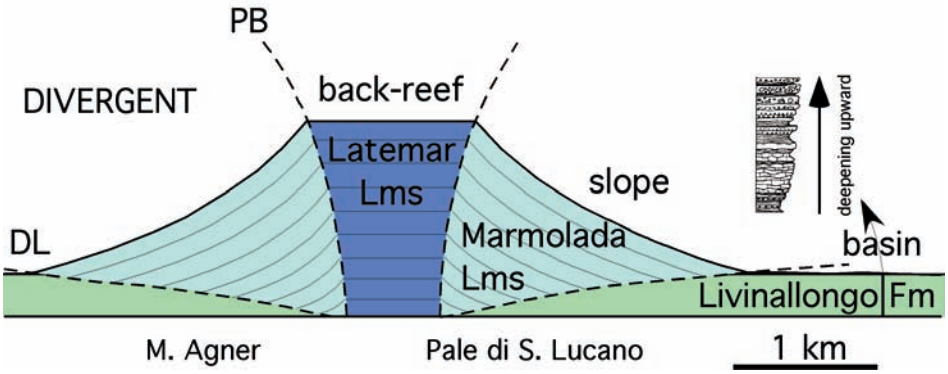

Fig. 206 - Reconstruction of the Ladinian Pale di San Lucano platform; NNW is to the right. Example of divergent platform break (PB) and downlap (DP) planes. Note that the basinal Livinallongo Formation shows a deepening upward sequence (1, black, laminated siliceous mudstone, starved basin; 2, nodular limestone; 3, graded calcarenites organized in small thickening-coarsening upward sequences). The Sciliar Dolomite (or Marmolada Limestone) is represented by megabreccias of the slope, whereas the Latemar Limestone consists of peritidal back-reef sediments (after DOGLIONI & BOSELLINI, 1989). The steep platform break is controlled by fast subsidence rate. It cannot be generated only by sea-level rise since the platform sequence is thicker than 1 km.

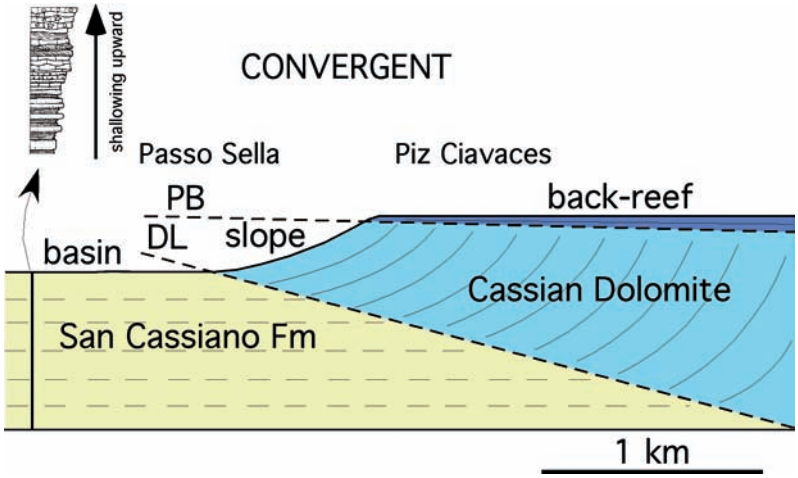

Fig. 207 - Reconstruction of the western margin of the Sella Carnian carbonate platform (Upper Cassian Dolomite). It is an example of convergence between the platform break plane (PB) and the downlap plane (DL). The coeval basin (San Cassiano Formation) consequently shows a shallowing upward sequence (1, graded calcarenites and breccias alternating with shale and mudstone; 2, nodular and wavy bedded limestones with traction-current structures; 3, wave bedded calcarenites). The flat and gentle dip of the platform break has to be related to absent or low subsidence rate.

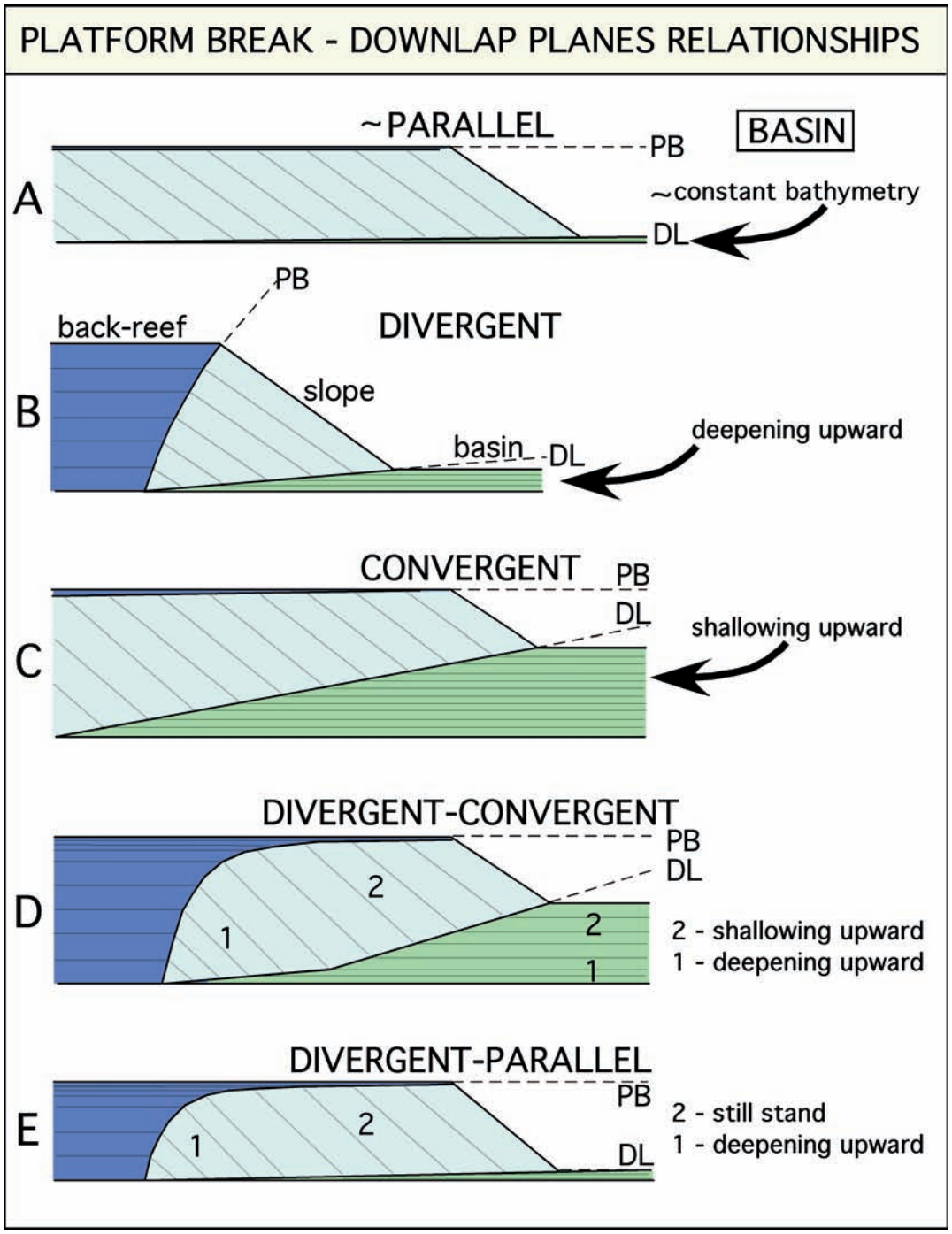

Fig. 208 - Different relationships between platform break and downlap planes in progradational systems produce different evolutions of the basin. A, parallel - constant bathymetry; B, divergent - deepening upward; C, convergent - shallowing upward; D, divergent-convergent - deepening and subsequent shallowing upward; E, divergent-parallel - deepening and subsequent still stand. PB, platform break plane; DL, downlap plane. The different kinds of geometries are principally controlled by subsidence rates, by sea-level eustatic oscillations, by carbonate productivity and by terrigenous input into the basin. Since subsidence and terrigenous input were variable from region to region in the Dolomites, during the same eustatic cycle carbonate platforms developed with different relationships between platform break and downlap planes (either convergent or divergent). For example, the Ladinian carbonate platforms of the Pale di San Lucano (B-type) and of the Catinaccio (E-type) developed contemporaneously in zones characterised by different subsidence (smaller, at a certain period, in the Catinaccio).

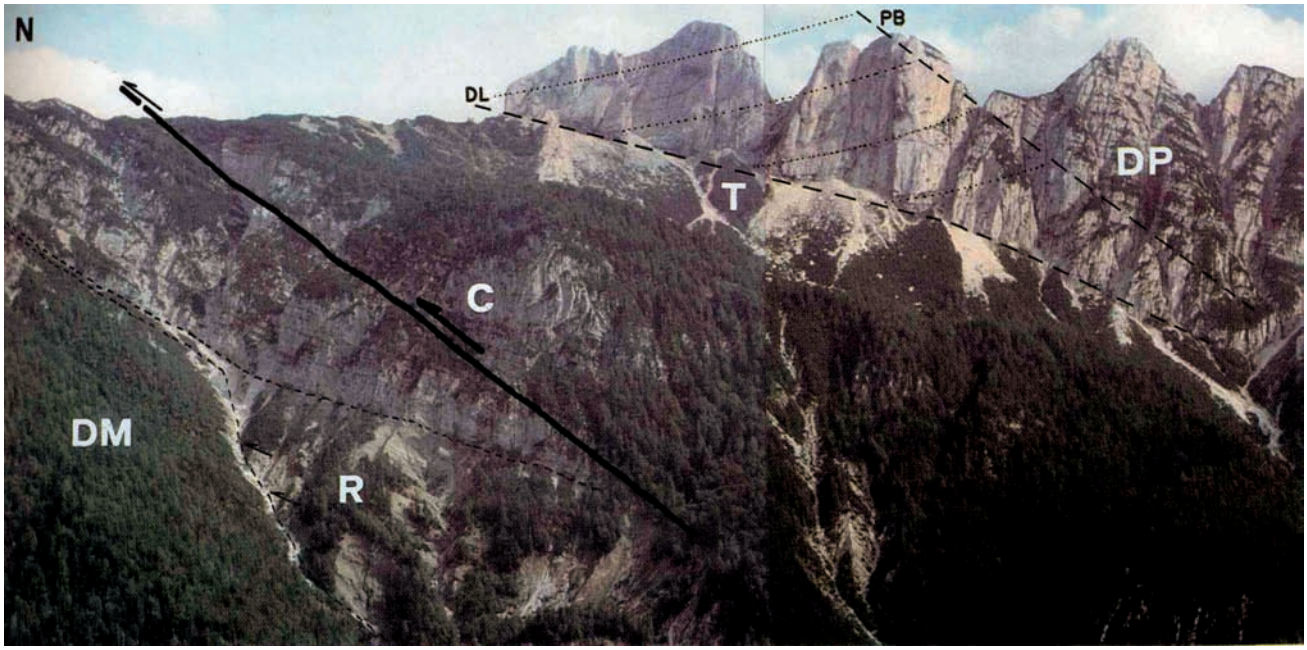

Fig. 209 - Natural section west of Raibl, in the Tarvisio area, between Portella and Mt. Guarda, to the right (eastern Southern Alps). DM, Ladinian Dolomia Metallifera, equivalent to the Sciliar Dolomite; R, Rio del Lago Fm, lower Carnian, consisting of marls and marly limestones onlapping the slope of the underlying platform (Dolomia Metallifera); C, Conzen Dolomite, middle Carnian; T, Tor Fm, upper Carnian, basinal equivalent of the upper Carnian-Norian Dolomia Principale (DP), consisting of classical peritidal dolomite to the right and of clinostratified megabreccias and calcarenites prograding towards the north in the central part of the picture. DL, Downlap plane; PB, Platform break plane.

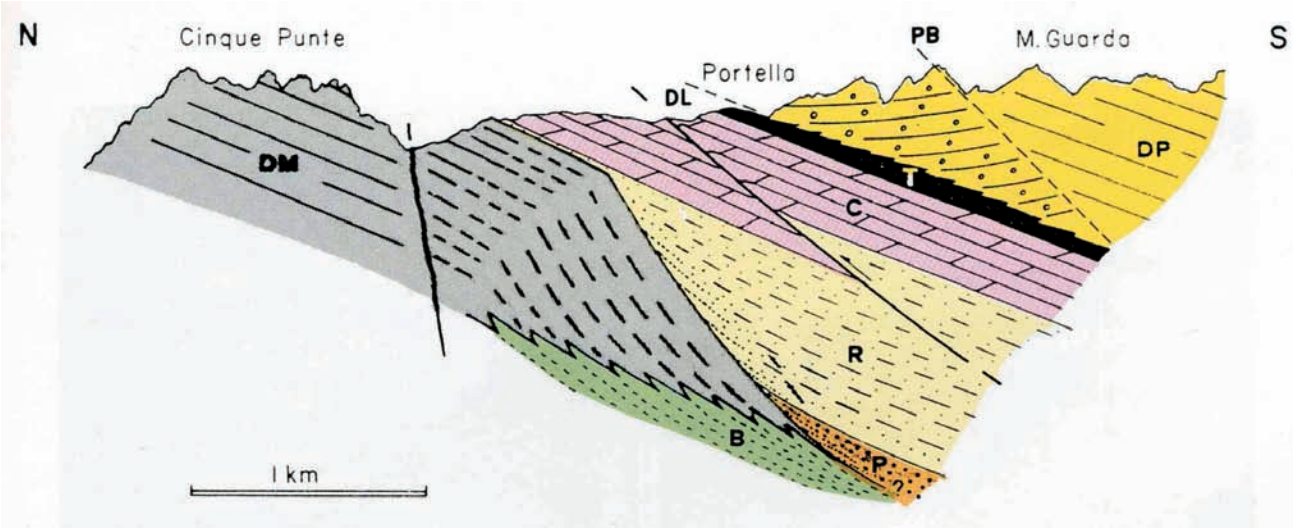

Fig. 210 - Section to the west of Raibl, Tarvisio area, between Cinque Punte and Mt. Guarda. DM, Dolomia Metallifera, Ladinian carbonate platform; B, Buchenstein (Livinallongo) Fm, Ladinian, basinal equivalent of the Dolomia Metallifera. P, Predil Limestone, lower Carnian; R, Rio del Lago Fm, lower Carnian, consisting of marls and marly limestones onlapping the slope of the underlying platform (Dolomia Metallifera); C, Conzen Dolomite, middle Carnian; T, Tor Fm, upper Carnian, basinal equivalent of the upper Carnian-Norian Dolomia Principale (DP), consisting of classical peritidal dolomite to the right and of clinostratified megabreccias and calcarenites prograding towards the north onto the Tor Fm; DL, Downlap plane; PB, Platform break plane. The picture of the previous figure represents the central-right part of the section.

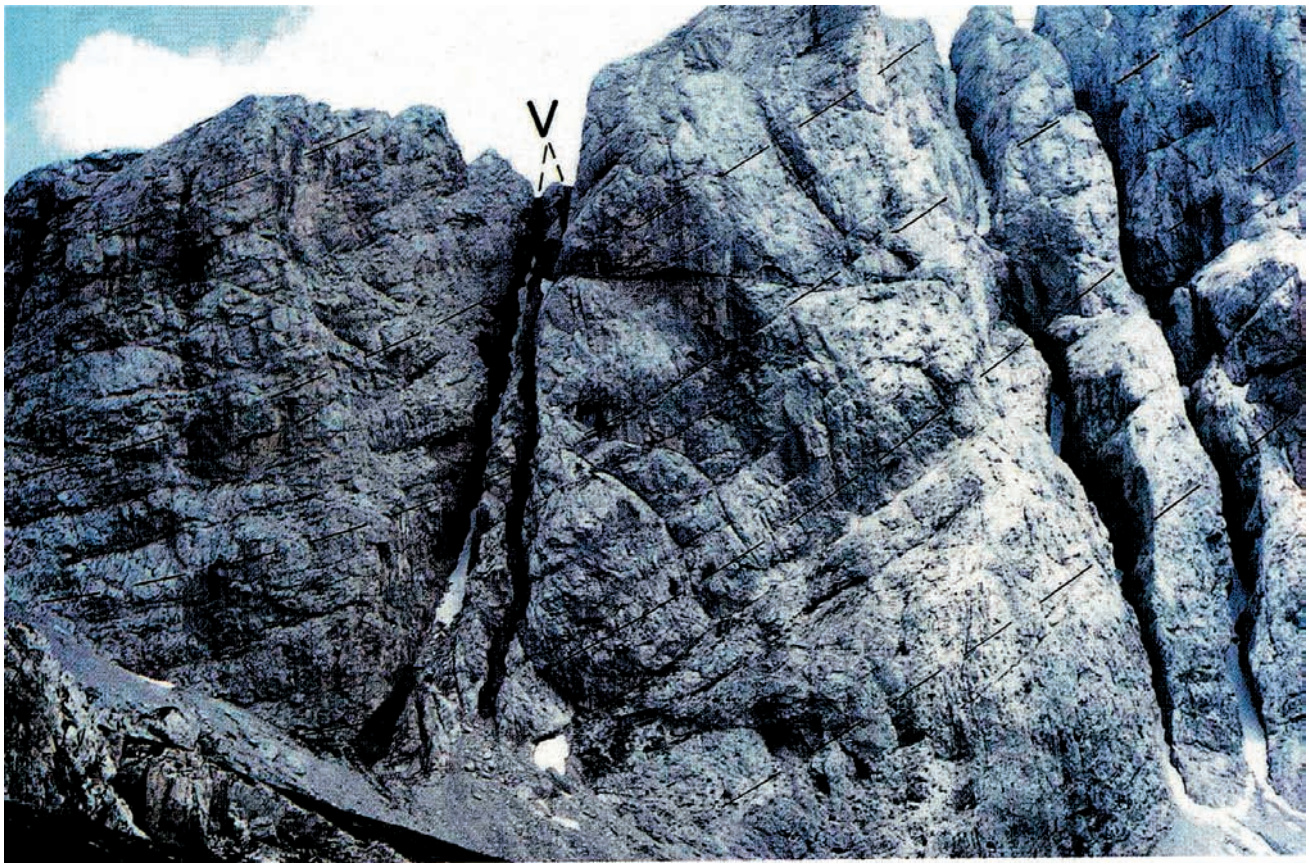

Fig. 211 - Clinostratifications of the prograding megabreccias of the Ladinian Sciliar Dolomite, observable along the northern flank of the Cime di Focobon. Some latite-basaltic dykes (V) referred to the upper Ladinian volcanic event cut the platform sediments.

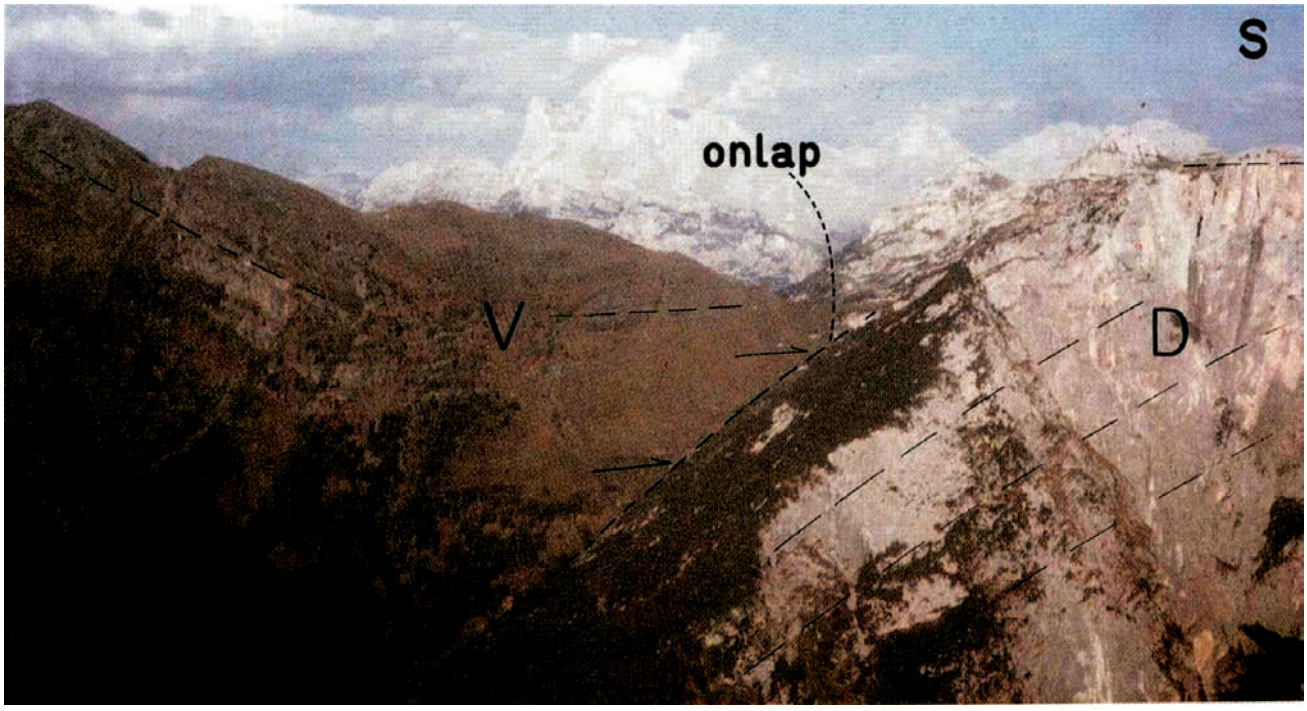

Fig. 212 - The famous onlap of the volcanic and volcaniclastic deposits (V) of Ladinian age onto the northern slope of the lower-middle Ladinian carbonate platform (D) of the Pale di San Lucano prograding towards the north, at the head of the Gares Valley.

Fig. 213 - Pillow lava of the Ladinian shoshonitic volcanic event in the Dolomites. Locality Colcuc, Andrè Droxler for scale.

Fig. 214 - Ladinian latit-basalt pillows covered (left) or lying on (right) and squeezing volcaniclastic turbidites. Locality Colcuc.

Fig. 215 - Caotico Eterogeneo, Ladinian mass flow deposit containing pebbles from the Upper Permian to the Ladinian. Volcanic rocks, basinal and platform fragments are included. Some elements are sheared or folded, and contained in the undeformed conglomerate, indicating Middle Triassic tectonics. Locality Lasta, Valle di Livinallongo.

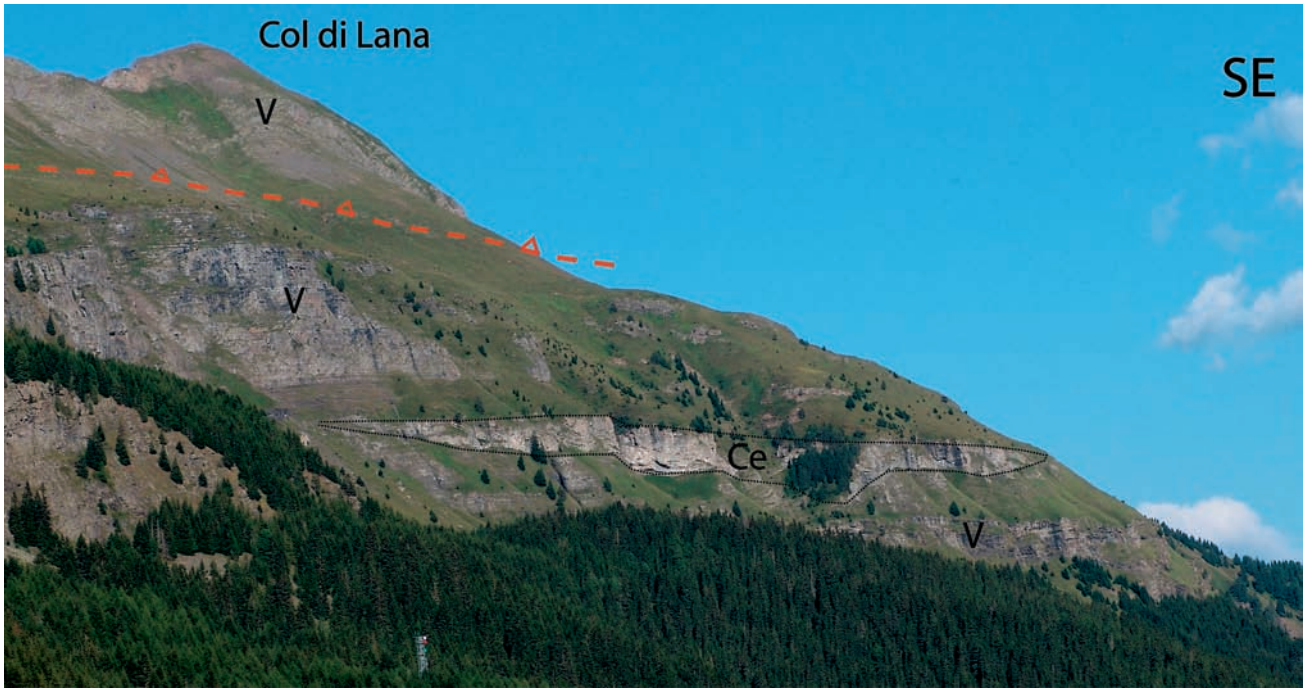

Fig. 216 - The Caotico Eterogeneo (Ce) occurs in channelized bodies interbedded in the turbiditic volcanoclastic sandstones of Ladinian age (V). This is an example in the Livinallongo Valley, in the southern slope of the Col di Lana, where the top is folded and thrusting toward the observer.

Fig. 217 - Carbonatic olistholith (Marmolada Limestone) included in the Upper Ladinian volcanic Marmolada Conglomerate. Road from Arabba to Passo Pordoi. Matteo Minervini, Elena Capoferri, David Hearty, Grant Ellis and others for scale.

Fig. 218 - Prograding Cassian Dolomite (D) of the Gardenaccia Massif over the San Cassiano Fm (S), toward the Val Badia. R, Raibl Fm; DP, Dolomia Principale.

Fig. 219 - Early Carnian San Cassiano Fm at Passo Sella. Carbonatic and volcanoclastic turbidites interfingered with emipelagic shales and marls. This basinal formation is eteropic to the Cassian Dolomite in the background. Silvia Campobasso, Cecile Huet, Eleonora Vitagliano, Daniele Fragola and others for scale.

Fig. 220 - Undolomitized olistholith of the Cassian Dolomite carbonate plaform included in a coarse grained (volcaniclastic rich) turbiditic facies of the San Cassiano Fm, Passo Sella. Casey Moore for scale.

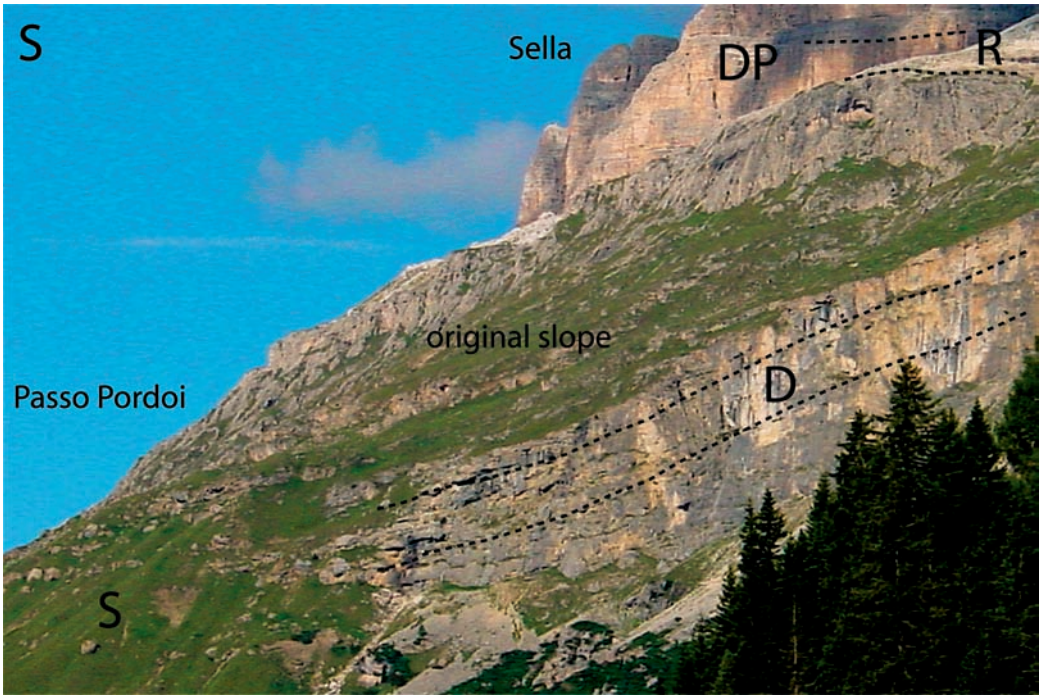

Fig. 221 - Interfingering between the clinoformed megabreccias of the Cassian Dolomite (D), representing the slope, and the basin of the San Cassiano Fm (S) in the green. R, Raibl Fm; DP, Dolomia Principale.

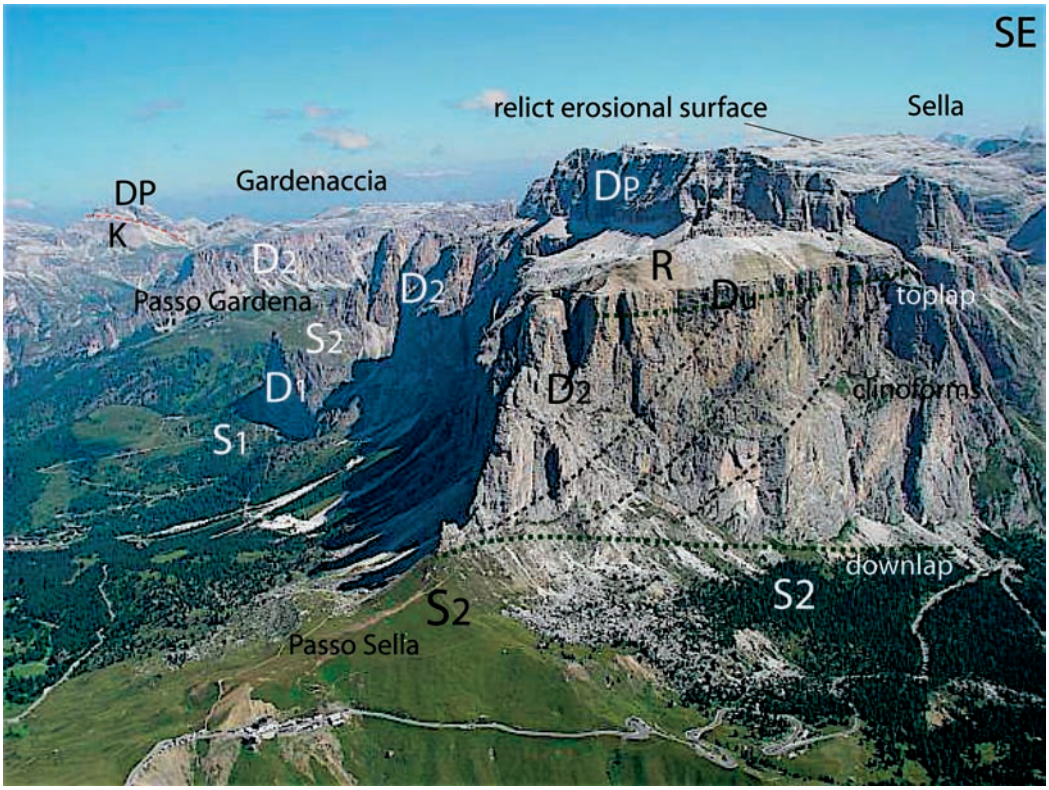

Fig. 222 - Stratigraphy of the western margin of the Sella Massif, central Dolomites. DP, Norian tidal flat Dolomia Principale; R, Upper Carnian Raibl Fm; Du, Carnian shallow water lagoon facies Dürrenstein Dolomite; D2, prograding megabreccias of the Carnian Upper Cassian Dolomite. S2, basinal sediments of the Carnian Upper San Cassiano Fm. In the background to the north toward Passo Gardena, D1, megabreccias of the Carnian Lower Cassian Dolomite, S1, the basinal sediments of the Lower San Cassiano Fm. In the Gardenaccia massif, the Dolomia Principale overrides the Cretaceous Puez Marls (K). Picture by Ulrich Prinz taken from a paraglide.

Fig. 223 - Carnian-Norian transition in the Mt. Faloria, southeast of Cortina. DP, Norian tidal flat Dolomia Principale; R, Upper Carnian Raibl Fm, here reddish, tidal flat and including some evaporites; Du, Carnian shallow water lagoon facies Dürrenstein Dolomite; D, megabreccias of the Carnian Cassian Dolomite.

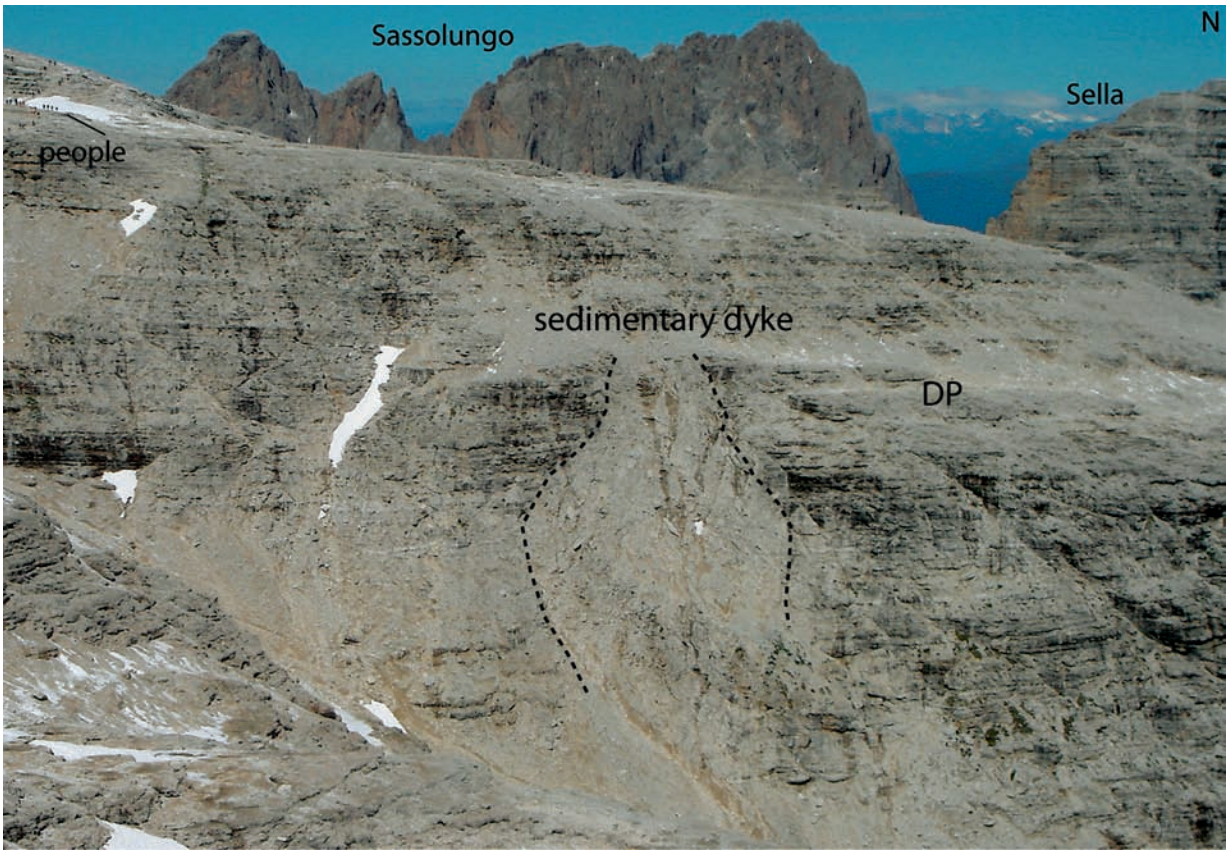

Fig. 224 - Intraformational sedimentary dyke in the Dolomia Principale (DP) near Sass Pordoi in the Sella Massif.